2014

Sensitivity analysis frameworks for mechanistic-empirical pavement design of continuously reinforced concrete pavements

Halil Ceylan
Iowa State University, hceylan@iastate.edu

Sunghwan Kim
Iowa State University, sunghwan@iastate.edu

Kasthurirangan Gopalakrishnan
Iowa State University, rangan@iastate.edu

See next page for additional authors

Sensitivity analysis frameworks for mechanistic-empirical pavement design of continuously reinforced concrete pavements

Abstract

The new AASHTO Mechanistic-Empirical Pavement Design Guide (MEPDG) performance predictions for the anticipated climatic and traffic conditions depend on the values of the numerous input parameters that characterize the pavement materials, layers, design features, and condition. This paper proposes comprehensive local sensitivity analyses (LSA) and global sensitivity analyses (GSA) methodologies to evaluate continuously reinforced concrete pavement (CRCP) performance predictions with MEPDG inputs under various climatic and traffic conditions. A design limit normalized sensitivity index (NSI) was implemented in both LSA and GSA to capture quantitative as well as qualitative sensitivity information. The GSA varied all inputs simultaneously across the entire problem domain while the LSA varied each input independently in turn. Correlations among MEPDG inputs were considered where appropriate in GSA. Two response surface modeling (RSM) approaches, multivariate linear regressions (MVLR) and artificial neural networks (ANN or NN), were developed to model the GSA results for evaluation of MEPDG CRCP input sensitivities across the entire problem domain. The ANN-based RSMs not only provide robust and accurate representations of the complex relationships between MEPDG inputs and distress outputs but also capture the variation of sensitivities across the problem domain. The NSI proposed in LSA and GSA provides practical interpretation of sensitivity relating a given percentage change in a MEPDG input to the corresponding percentage change in predicted distress relative to its design limit value. The "mean plus/minus two standard deviations (Î¼ + 2Ïƒ)" GSA-NSI metric (GSA-NSIÎ¼ Â±2Ïƒ) derived from ANN RSM statistics is the best and most robust design input ranking measure since it incorporates both the mean sensitivity and the variability of sensitivity across the problem domain.

Keywords

AASHTO, concrete, design, pavement, sensitivity analyses

Disciplines

Civil and Environmental Engineering | Construction Engineering and Management

Comments

NOTICE: This is the author's version of a work that was accepted for publication in *Construction and Building Materials*. Changes resulting from the publishing process, such as peer review, editing, corrections, structural formatting, and other quality control mechanisms may not be reflected in this document. Changes may have been made to this work since it was submitted for publication. A definitive version was subsequently published in *Construction and Building Materials* 73 (2014): doi: 10.1016/j.conbuildmat.2014.09.091.

Authors

Halil Ceylan, Sunghwan Kim, Kasthurirangan Gopalakrishnan, Charles W. Schwartz, and Rui Li

Reference to this paper should be made as follows: Ceylan, H., Kim, S., Gopalakrishnan, K., Schwartz, C. W., and Li, R. (2014). "*Sensitivity Analysis Frameworks for Mechanistic-Empirical Pavement Design of Continuously Reinforced Concrete Pavements*," Construction and Building Materials. Vol. 73, pp. 498–508.

Sensitivity Analysis Frameworks for Mechanistic-Empirical Pavement Design of Continuously Reinforced Concrete Pavements

Halil Ceylan[1], Sunghwan Kim[2], Kasthurirangan Gopalakrishnan[3], Charles W. Schwartz[4], and Rui Li[5]

[1]Associate Professor, 406 Town Engineering Building, Department of Civil, Construction and Environmental Engineering, Iowa State University, Ames, IA 50011, USA, Phone: 1-515-294-8051, Fax: 1-515-294-8216, E-mail: hceylan@iastate.edu

[2]Research Assistant Professor (Corresponding Author), 24 Town Engineering Building, Department of Civil, Construction and Environmental Engineering, Iowa State University, Ames, IA 50011, USA, Phone: 1-515-294-4698, Fax: 1-515-294-8216, E-mail: sunghwan@iastate.edu

[3]Research Associate Professor, 354 Town Engineering Building, Department of Civil, Construction and Environmental Engineering, Iowa State University, Ames, IA 50011, USA, Phone: 1-515-294-3044, Fax: 1-515-294-8216, E-mail: rangan@iastate.edu

[4]Professor, 0147C Glenn L. Martin Hall, Department of Civil and Environmental Engineering, University of Maryland, College Park, MD 20742, Phone: 1-301-405-1962, Fax: 301-405-2585, E-mail: schwartz@umd.edu

[5]Research Assistant, 0147C Glenn L. Martin Hall, Department of Civil and Environmental Engineering, University of Maryland, College Park, MD 20742, Phone: 1-703-953-4335, Fax: 301-405-2585, E-mail: lirui@umd.edu

Reference to this paper should be made as follows: Ceylan, H., Kim, S., Gopalakrishnan, K., Schwartz, C. W., and Li, R. (2014). "*Sensitivity Analysis Frameworks for Mechanistic-Empirical Pavement Design of Continuously Reinforced Concrete Pavements*," Construction and Building Materials. Vol. 73, pp. 498–508.

Abstract

The new AASHTO Mechanistic-Empirical Pavement Design Guide (MEPDG) performance predictions for the anticipated climatic and traffic conditions depend on the values of the numerous input parameters that characterize the pavement materials, layers, design features, and condition. This paper proposes comprehensive local sensitivity analyses (LSA) and global sensitivity analyses (GSA) methodologies to evaluate continuously reinforced concrete pavement (CRCP) performance predictions with MEPDG inputs under various climatic and traffic conditions. A design limit normalized sensitivity index (NSI) was implemented in both LSA and GSA to capture quantitative as well as qualitative sensitivity information. The GSA varied all inputs simultaneously across the entire problem domain while the LSA varied each input independently in turn. Correlations among MEPDG inputs were considered where appropriate in GSA. Two response surface modeling (RSM) approaches, multivariate linear regressions (MVLR) and artificial neural networks (ANN or NN), were developed to model the GSA results for evaluation of MEPDG CRCP input sensitivities across the entire problem domain. The ANN-based RSMs not only provide robust and accurate representations of the complex relationships between MEPDG inputs and distress outputs but also capture the variation of sensitivities across the problem domain. The *NSI* proposed in LSA and GSA provides practical interpretation of sensitivity relating a given percentage change in a MEPDG input to the corresponding percentage change in predicted distress relative to its design limit value. The "mean plus/minus two standard deviations (μ+2σ)" GSA-NSI metric (GSA-NSI$_{\mu\pm2\sigma}$) derived from ANN RSM statistics is the best and most robust design input ranking measure since it incorporates both the mean sensitivity and the variability of sensitivity across the problem domain.

Keywords: Concrete; Pavement; Sensitivity Analyses; Design; AASHTO

Reference to this paper should be made as follows: Ceylan, H., Kim, S., Gopalakrishnan, K., Schwartz, C. W., and Li, R. (2014). "*Sensitivity Analysis Frameworks for Mechanistic-Empirical Pavement Design of Continuously Reinforced Concrete Pavements*," Construction and Building Materials. Vol. 73, pp. 498–508.

1. Introduction

The AASHTOWare Pavement ME Design [1] was developed to more realistically represent changes in current material properties, traffic loading variations, climatic effects and role of construction in the pavement design procedure. It builds upon the Mechanistic-Empirical Pavement Design Guide (MEPDG) resulting from the National Cooperative Highway Research Program (NCHRP) 1-37A project [2] and AASHTO MEPDG Manual of Practice [3] for providing pavement analysis and performance predictions under various "what-if" scenarios.

There is no doubt that MEPDG could upgrade the efficiency of pavement analysis and designs. However, it requires a fully understanding of over 50 pavement design inputs which are higher than previous pavement design procedures. The performance predictions (i.e., MEPDG outputs) for the anticipated climatic and traffic conditions will depend on the values of these input parameters that characterize the pavement materials, layers, design features, and condition. The MEPDG performance predictions for continuously reinforced concrete pavement (CRCP) include punchout, crack width, crack load transfer efficiency (LTE), and IRI. Knowledge of the sensitivity of predicted performance to the MEPDG input values can help identify, for specific climatic region and traffic load conditions, the inputs that most influence predicted performance. This will help pavement designers determine where additional effort is justified in developing higher quality and/or more certain input values.

MEPDG sensitivity studies for rigid pavements began appearing in the literature immediately after the initial release of the MEPDG in 2004. Detailed discussions by Schwartz et al. [4] on procedures employed by previous studies and related findings indicate that the previous MEPDG sensitivity studies have been limited in scope, approach, and findings. These limitations include varying only small subsets of inputs, reliance on sensitivity analysis approaches without answering the question that "if input x goes up by n%, output y goes down by m%", neglecting any correlations and/or interactions among input parameters, fewer studies focusing on CRCP performance predictions, and analysis using earlier versions of the MEPDG software and models which are different from the latest version of MEPDG software (version 1.1) that form the main framework of AASHTOWare Pavement ME Design.

The objective of this study, a subset of the NCHRP Project 1-47 "Sensitivity Evaluation of MEPDG Performance Prediction", is to quantify the sensitivity of MEPDG CRCP performance predictions to MEPDG input variations. To avoid the limitations associated with the previous MEPDG sensitivity studies, this study proposes local sensitivity analysis (LSA) and global sensitivity analysis (GSA) approaches with the use of a design limit normalized sensitivity index (NSI) to provide both quantitative and qualitative sensitivity information. By using the latest versions of MEPDG software (version 1.1), various CRCP sections representing new construction were designed for three traffic levels (low, medium, and high) in five climate zones (Hot-Wet, Hot-Dry, Cold-Wet, Cold-Dry, and Temperate) to assess sensitivity over the entire MEPDG parameter space. The procedures and the results from LSA and GSA are discussed in this paper highlighting the significant MEPDG input properties required for conducting routine MEPDG and AASHTOWare Pavement ME Design CRCP analysis and design.

2. Local and global sensitivity analysis

Sensitivity analysis is the apportionment of output variability from a model to its various inputs. Sensitivity analysis draws upon many of the same concepts as the design of experiments. A rich and powerful set of formal and rigorous techniques for performing sensitivity analyses has been developed over recent years [5, 6]. These can be categorized in a variety of ways. For the purposes of the present discussion, the most useful categorizations are LSA and GSA methods. LSA provides an economical approach for identifying the subset of inputs that have the largest impact on the outputs. Only the sensitivities around the reference input values for the baseline cases are evaluated—i.e., the evaluation is only for very small regions of the overall solution space. This provides only a "local" as opposed to a "global" sensitivity evaluation. The one-at-time (OAT) method is the most common type of LSA. In standard OAT applications, one or more baseline scenarios are exercised by varying each input independently in turn.

In GSA approach, not only is the local sensitivity around a specific point in the parameter space evaluated, but an attempt is made to assess this sensitivity over the entire parameter space as all input parameters are varied simultaneously. GSA can include input correlations and interactions which LSA ignores. To quantify the level of sensitivity, the sensitivity metrics employed in this study include LSA sensitivity index and GSA sensitivity index statistics. Sensitivity index statistics here refer to full frequency distributions of sensitivity index. Detailed descriptions of both sensitivity index and sensitivity index statistics are presented in the following sections.

3. LSA methodology for MEPDG

One-at-a-time LSA were performed to identify preliminary triage of MEPDG inputs for GSA analysis to confirm high sensitivity input factors that need to be included in the GSA and identify any potential correlations of inputs. Fig. 1 is a schematic of the overall OAT LSA used in this study.

Sensitivity analyses were conducted for the full ranges of all model inputs and outputs. However, not all combinations of model input values are physically plausible. For example, a thick rigid pavement on stiff foundation subjected to low traffic volume does not represent a realistic scenario likely to be encountered in practice. Therefore, a set of base cases were made for both of OAT LSA and GSA to cover the ranges of commonly encountered pavement types, climate conditions and traffic levels. The MEPDG design inputs varied in the OAT LSA were prepared and utilized in MEPDG simulations. MEPDG simulations in OAT LSA were conducted for baseline, minimum, and maximum values of each design input. Using MEPDG design inputs and performance predictions, sensitivity indices were calculated to determine levels of sensitivity. A detailed procedure of OAT LSA is discussed in next subsection.

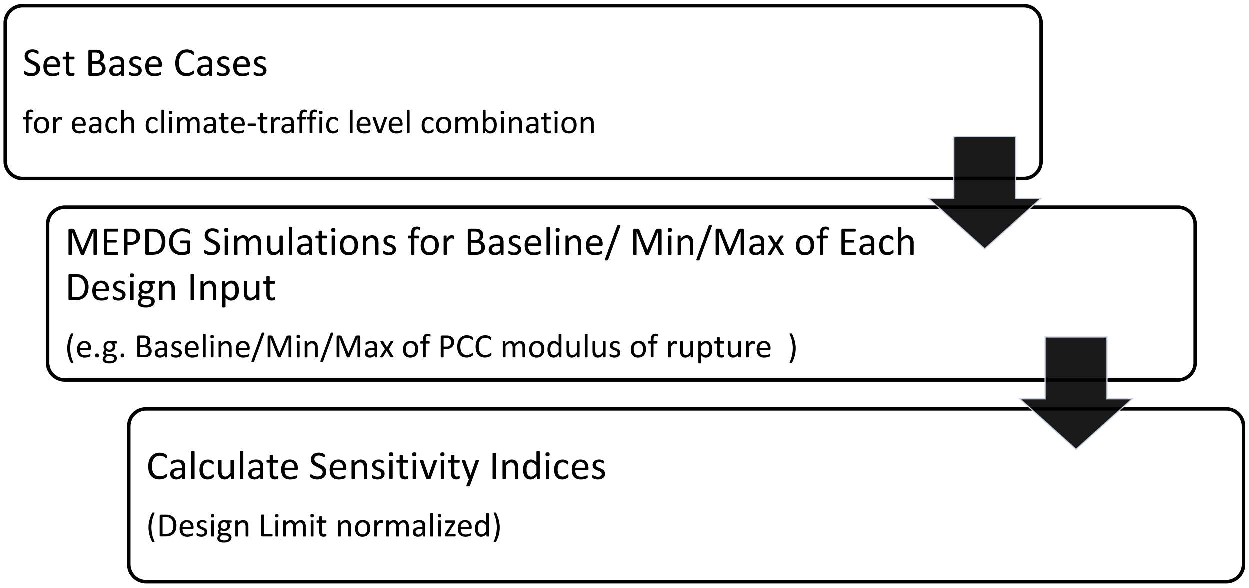

Fig. 1. The schematic of the overall OAT LSA approach.

3.1. Base cases

The OAT LSA of CRCP encompassed a total of 15 base cases with five climatic zones and three traffic levels. The five representative climatic zones in the United States utilized for base case analysis include hot-dry (HD), hot-wet (HW), temperate (T), cold-dry (CD) and cold-wet (CW). Table 1(a) summarizes the specific locations and the weather stations used to generate the climate files for each of the five climatic zones. The three traffic levels used in all OAT LSA are summarized in Table 1(b). The ranges of average annual daily truck traffic (AADTT) for the three traffic levels are listed similar to truck volume categories from Alam et al [7]. To put these traffic volumes into a more familiar context, the approximate numbers of equivalent single axle loads (ESALs) are also included in Table 1(b). The baseline values with ranges of the Portland Cement Concrete (PCC) slab and base thickness inputs for each the traffic category are also listed in Table 1(b). Higher traffic levels require correspondingly thicker PCC and base layers.

Details of the traffic input such as vehicle class distributions, axle load distributions, seasonal and daily traffic distributions, axle geometric configuration, tire pressure, and traffic growth rates were not considered in this study.

Reference to this paper should be made as follows: Ceylan, H., Kim, S., Gopalakrishnan, K., Schwartz, C. W., and Li, R. (2014). "*Sensitivity Analysis Frameworks for Mechanistic-Empirical Pavement Design of Continuously Reinforced Concrete Pavements*," Construction and Building Materials. Vol. 73, pp. 498–508.

Table 1. Categories for base cases: (a) climate; (b) traffic and CRCP thickness ranges.

(a)

Climate Category	Location	Weather Station	Mean annual air temperature (ºC)	Min temperature (ºC)	Max temperature (ºC)	Mean annual rainfall (mm)
Hot-Wet	Orlando, FL	ORLANDO INTERNATIONAL ARPT	22.0	11.3	31.8	1,271
Hot-Dry	Phoenix, AZ	PHOENIX SKY HARBOR INTL AP	23.9	11.9	35.7	171
Cold-Wet	Portland, ME	PORTLAND INTL JETPORT ARPT	8.3	-4.7	22.1	999
Cold-Dry	International Falls, MN	FALLS INTERNATIONAL ARPT	4.2	-13.0	19.7	642
Temperate	Los Angeles, CA	LOS ANGELES INTL AIRPORT	10.1	10.1	26.9	360

(b)

Traffic Level	Low Traffic			Medium Traffic			High Traffic		
Input Parameter	**Baseline**	**Min**	**Max**	**Baseline**	**Min**	**Max**	**Baseline**	**Min**	**Max**
AADTT- Nominal[1]	1,000	500	5,000	7,500	5000	10,000	25,000	20,000	30,000
AADTT- Design Lane[2]	375	188	1,875	2,063	1,375	2,750	6,250	5,000	7,500
Est. ESALs[2]	5M	2M	20M	25M	20M	35M	75M	60M	90M
PCC, mm	203	178	229	254	203	305	305	254	356
Base, mm	102	51	152	152	102	203	203	152	254

[1]Based on MEPDG Interstate Highway TTC4 Level 3 default vehicle distribution/two lanes for low traffic and three lanes for medium and high traffic.

[2]50% directional split, 2 lanes per direction, 0.75 lane factor for design lane on low traffic/50% directional split, 3 lanes per direction, 0.55 lane factor for design lane on medium traffic/50% directional split, 3 lanes per direction, 0.50 lane factor for design lane on high traffic.

3.2. Analysis inputs

The MEPDG CRCP inputs varied in the OAT LSA simulations are summarized in Table 2. These inputs were identified as the sensitive MEPDG CRCP inputs through combination of insights from prior acceptable sensitivity studies and consensus engineering judgment of the sensitivity of the distress to each MEPDG design input. The detailed procedures and results of these combined sensitivity assessments are provided in Schwartz et al. [4]. The baseline, minimum and maximum value used in OAT LSA were listed for each design input.

The edge support input in MEPDG CRCP analyses are given as four shoulder types including asphalt, gravel, monolithic tied concrete, and separate tied concrete. Each shoulder type is represented here in terms of its equivalent LTE value. The MEPDG requires that the maximum steel depth be equal to PCC slab mid-depth. Therefore, the baseline and ranges of steel depth values were changed in accordance with PCC slab thickness under each traffic level. A water-to-cement (W/C) ratio of 0.4 was used as the baseline value in OAT LSA analyses.

The MEPDG uses an explicit hierarchical approach for the designer to flexibly select design inputs based on the relative importance, size, cost, and available resources of the project. A total of six design input options (Leve1 1, Level 2, and the four Level 3 alternatives) are available in the MEPDG for PCC stiffness and strength in CRCP. Level 1 of the MEDPG requires measured values of PCC elastic modulus (E), modulus of rupture (MOR), and indirect tensile strength (ITS) at various ages to characterize stiffness and strength gains over time. The required stiffness and strength values at Level 2 are estimated from compressive strength (f_c') results at various ages. Corresponding values of E, MOR, and ITS are estimated from f_c' using standard empirical relations [8]. The required stiffness and strength values at Level 3 are estimated from a single point measurement of MOR (or f_c') and optionally the corresponding measured E at 28 days. The four options for specifying Level 3 PCC stiffness and strength design inputs are (1) the measured 28-day MOR only; (2) the measured 28-day f_c' only; (3) the measured 28-day MOR and the measured 28-day E; and (4) the measured 28-day f_c' and the measured 28-day E. Using these inputs, the MEPDG estimates stiffness and strength gains over time. It is obvious that Level 1 inputs require more detailed laboratory measurements for the highest accuracy.

A previously completed study [9] indicated that the Level 3 input combination of measured 28-day MOR and measured 28-day E predicted distresses that were consistently in closest agreement with predictions using Level 1 inputs. . The Level 3 inputs pertaining to measured 28-day MOR and E were utilized in the OAT LSA analyses.

Reference to this paper should be made as follows: Ceylan, H., Kim, S., Gopalakrishnan, K., Schwartz, C. W., and Li, R. (2014). "*Sensitivity Analysis Frameworks for Mechanistic-Empirical Pavement Design of Continuously Reinforced Concrete Pavements*," Construction and Building Materials. Vol. 73, pp. 498–508.

Table 2. MEPDG CRCP input parameter ranges.

Input Parameter	**Baseline**	**Minimum**	**Maximum**
Construction Month	Jul-06	Mar-06	Oct-06
Bar Diameter, mm	15.2	12.7	25.4
Percent Steel, %	0.75	0.5	1
Steel Depth, mm	84,102,127/Various[1]	Base× 0.9 /64[1]	Base× 1.1 /178[1]
Edge Support – Load Transfer Efficiency, %	5 (Asphalt or Gravel)	5	70(Tied PCC)
Base Slab Friction Coefficient	2.5	0.5	4
Surface Shortwave Absorption	0.85	0.8	0.98
PCC Unit Weight, kg/m^3	2,403	2,243	2,563
PCC Poisson's Ratio	0.15	0.1	0.2
PCC Coef. of Thermal Expansion (mm/mm-^{o}C)	10.0	3.6	18.0
PCC Cement Content, kg/m^3	297	237	415
PCC Water-to-Cement Ratio	0.4/Various[1]	0.3	0.7
PCC 28-Day Modulus of Rupture, kPa	4,275	3,103	6,067
PCC 28-Day Elastic Modulus, MPa	27,280	16,068	42,591
PCC 28-Day Indirect Tensile Strength, kPa	2,861	1,868	4,475
PCC Ratio of 20-year to 28-day Modulus of Rupture	1.2	1	1.5
PCC Ratio of 20-year to 28-day Indirect Tensile Strength	1.2	1	1.5
Base Resilient Modulus, MPa	172	103	276
Subgrade Resilient Modulus, MPa	103	69	138
Groundwater Depth, m	3.0	0.6	5.5

[1]For OAT LSA/For GSA

3.3. MEPDG OAT LSA simulations

The design inputs in Table 1 and Table 2 were varied over 3 input levels (baseline, minimum, and maximum) for 15 base cases (5 climate zones and 3 traffic levels) in the OAT LSA sensitivity analyses. This requires a total of 585 MEPDG runs for the CRCP scenarios. The predicted distress levels for each of the CRCP baseline scenarios are summarized in Table 3. The predictions span a wide range of magnitudes for all distress predictions to the MEPDG recommended design limits.

Table 3. Predicted distress levels for CRCP baseline scenarios.

Traffic	Climate	PCC, mm	Base, mm	Crack Width, μm	Crack LTE, %	Punchout, per km	IRI, m/km
Low	Hot-Wet	203	102	422	93.2	1.7	1.08
Low	Hot-Dry	203	102	579	83.3	1.8	1.09
Low	Cold-Wet	203	102	528	88.1	2.0	1.39
Low	Cold-Dry	203	102	475	90.8	4.3	2.20
Low	Temperate	203	102	480	90.3	1.2	1.06
Medium	Hot-Wet	254	152	424	93.3	0.2	1.01
Medium	Hot-Dry	254	152	584	59.7	1.9	1.09
Medium	Cold-Wet	254	152	531	82.2	0.4	1.31
Medium	Cold-Dry	254	152	462	89.6	0.7	2.02
Medium	Temperate	254	152	485	86.9	0.2	1.00
High	Hot-Wet	305	203	455	87.8	0.1	1.00
High	Hot-Dry	305	203	620	44	12.5	1.62
High	Cold-Wet	305	203	569	49.6	4.7	1.52
High	Cold-Dry	305	203	500	69.3	0.9	2.02
High	Temperate	305	203	513	71.1	0.5	1.02
Recommended Design Limit				508	75	6.2	2.71

3.4. Sensitivity metrics for LSA

There is a wide variety of metrics that can be used to present level of sensitivity of model outputs to model inputs. This study implemented OAT LSA using a "design limit" *NSI* to provide both quantitative and qualitative sensitivity information. Note that quantitative sensitivity information here is the physical interpretation of sensitive analysis results and qualitative sensitivity information here is the ranking of sensitive input.

The *NSI* used in OAT LSA is S_{jk}^{DL} defined as:

$$S_{jk}^{DL} = \frac{\Delta Y_j}{\Delta X_k}\frac{X_k}{DL_j} \qquad (1)$$

in which X_k is the baseline value of design input k, ΔX_k is the change in design input k about the baseline, ΔY_j is the change in predicted distress j corresponding to ΔX_k, and DL_j is the design limit for distress *j*. For simplicity, the design limit NSI for OAT LSA, S_{jk}^{DL} is termed more simply as the "LSA normalized sensitivity index" or LSA- NSI.

The LSA-NSI always uses the design limit as the normalizing factor for the predicted distress. LSA-NSI can be interpreted as the percentage change in predicted distress relative to the design limit caused by a given percentage change in the design input. For example, consider CRCP punchouts as the predicted distress with a design limit of 6.2 per km (10 per mile). An NSI of 3.6 for the sensitivity of punchout predictions to AADTT implies that a 10% increases in AADTT will increase punchouts by $\Delta X_k \times NSI$ =36% of its design limit DL_j--i.e., it will increase punchouts by 0.10 (ΔX_k) × 3.6 (*NSI*) × 6.2 (design limit for CRCP punchouts) = 2.232 per km (3.6 per mile).

4. LSA results

The primary distresses predicted by the MEPDG for CRCP are punchouts and IRI. In the punchout model implemented in the MEPDG, an increase in crack width along with loss of support in the base leads to a degradation of LTE that facilitates the development of punchouts. Therefore, predicted crack width and crack LTE are calculated as part of punchout prediction procedure and reported in MEPDG outputs.

An *LSA- NSI* value was calculated for CRCP punchouts, crack width, crack LTE, and IRI for each of the base cases. The OAT LSA results for CRCP punchout and IRI are discussed here. Detailed OAT LSA results for CRCP crack width and LTE are presented in Schwartz et al. [4].

4.1. Punchout performance predictions

Fig. 2 presents the *LSA- NSI* values for punchouts. The variations of the *LSA- NSI* values resulting from different traffic and climate conditions are presented using error bars. PCC slab thickness and PCC MOR rank as the two most sensitive design inputs, with NSI values ranging from -6 to -37. This is in good agreement with engineering experience that an increase in structural capacity via increased slab thickness and strength will reduce punchout distress.

The next most sensitive design inputs include percent steel with LSA- NSI values varying from -10 to -23 and bar diameter with NSI values varying up to about 14. The increase in percent steel is highly effective in reducing punchouts due to tightly closed cracks and reduced loss of LTE. In general, as the bar diameter increases, the percent steel increases with consequent reduction in punchout distress. However, an increase in bar diameter under fixed steel percentage as in this OAT LSA analysis leads to increase in crack width with loss of crack LTE and consequent increase in punchout predictions.

Reference to this paper should be made as follows: Ceylan, H., Kim, S., Gopalakrishnan, K., Schwartz, C. W., and Li, R. (2014). "*Sensitivity Analysis Frameworks for Mechanistic-Empirical Pavement Design of Continuously Reinforced Concrete Pavements*," Construction and Building Materials. Vol. 73, pp. 498–508.

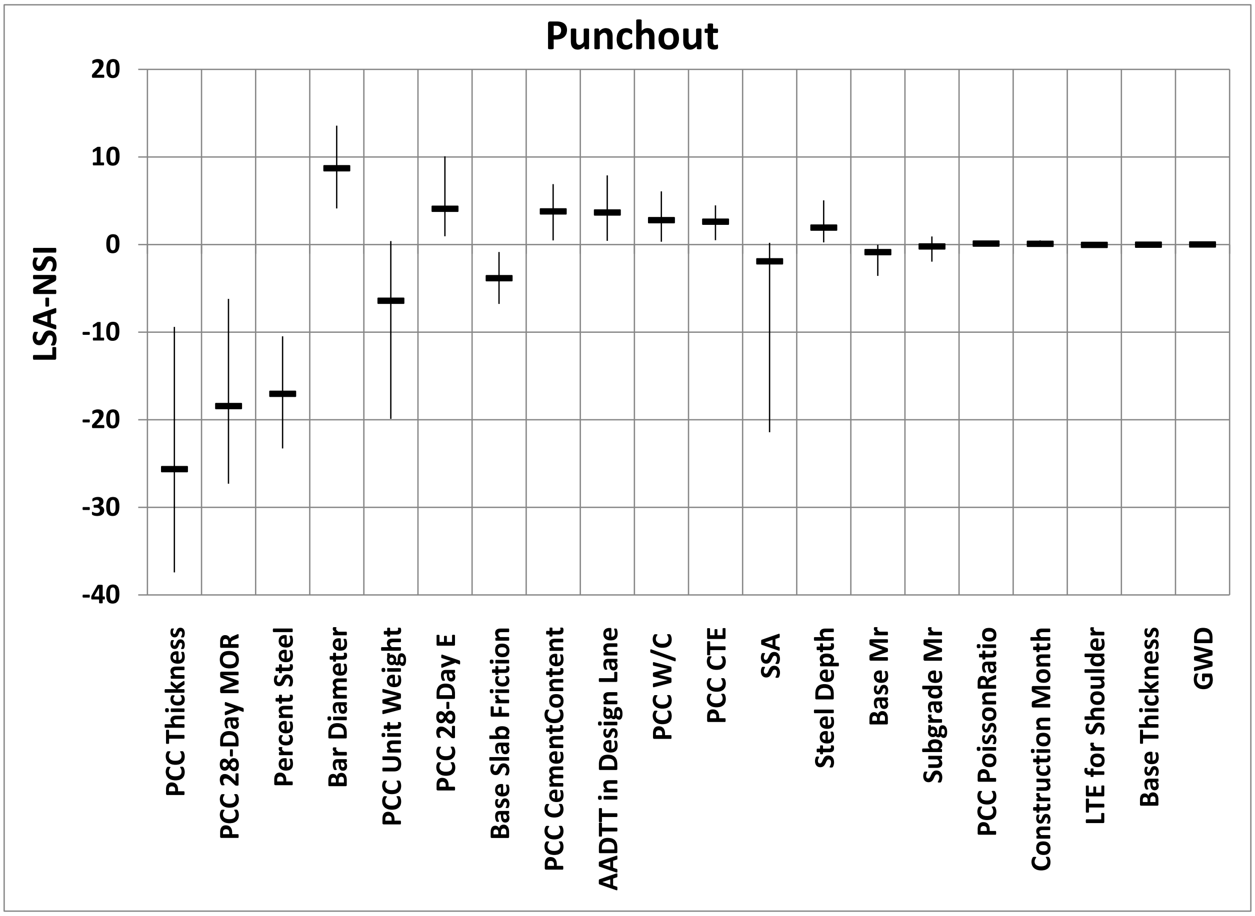

Fig. 2. LSA-NSI values for punchout in CRCP.

Other sensitive design inputs include PCC 28-day E, base/slab friction coefficient, PCC unit weight, PCC coefficient of thermal expansion (CTE), PCC cement content, PCC W/C ratio, AADTT, surface shortwave absorption (SSA), steel depth, base and subgrade resilient modulus (M_r). The following significant findings are noted:

- As PCC E increases, it leads to increased predicted punchouts due to higher bending stress. The use of base layers with high friction coefficients could reduce punchout distress by reducing mean crack spacing and providing tighter cracks.
- The PCC CTE and the PCC unit weight are used in the calculation of bending stress at the top surface of the CRCP slab in MEPDG. The calculated bending stress is one of the two input parameters for concrete fatigue equation of MPEDG punchout performance prediction model. The other input parameter is PCC MOR which is listed among most sensitive design inputs. Heavier PCC slab and lower PCC CTE are beneficial in minimizing slab curling and consequently mitigating punchout distress if all other design and construction parameters remain the same.
- PCC cement content and PCC W/C ratio are used in calculating the PCC zero stress temperature and ultimate shrinkage strain input parameters for the crack width predictive equations in MEPDG. Increased cement content and PCC W/C ratio lead to increases in crack width predictions and consequent increase in punchout predictions. Since SSA is

utilized in defining the temperature and moisture regime within the CRCP system in MEPDG, the different climate zone could lead to a wide range of LSA- NSI values of SSA for punchout predictions.

- Increase in steel depth from pavement surface to the center of reinforcing steel leads to increase in crack width increase and reduction in crack LTE which results in increase in punchout predictions.
- It is reasonable that higher AADTT produces more punchouts.
- A strong base and subgrade is beneficial in minimizing punchouts by reducing potential loss of support, but this effect is not strong in these OAT LSA analyses.

All other design inputs have average LSA-NSI values less than 0.5 (see Fig. 2). The low *NSI* values of these inputs means they have minor influence on predicted CRCP punchouts.

4.2. IRI performance predictions

The *LSA-NSI* values for IRI are summarized in Fig 3. Similar to IRI predictions for the other pavement types, IRI predictions in the CRCP cases are calculated from regression equations using primary distresses—punchouts, in the case of CRCP—as primary inputs along with a site factor and initial smoothness. The most sensitive design inputs for CRCP IRI predictions include PCC thickness, PCC 28-day MOR, percent steel, bar diameter, PCC unit weight, PCC 28-day E, base/slab friction coefficient, PCC cement content, AADTT, PCC W/C, PCC CTE, SSA, steel depth, base and subgrade M_r. These are also sensitive design inputs for CRCP punchout predictions.

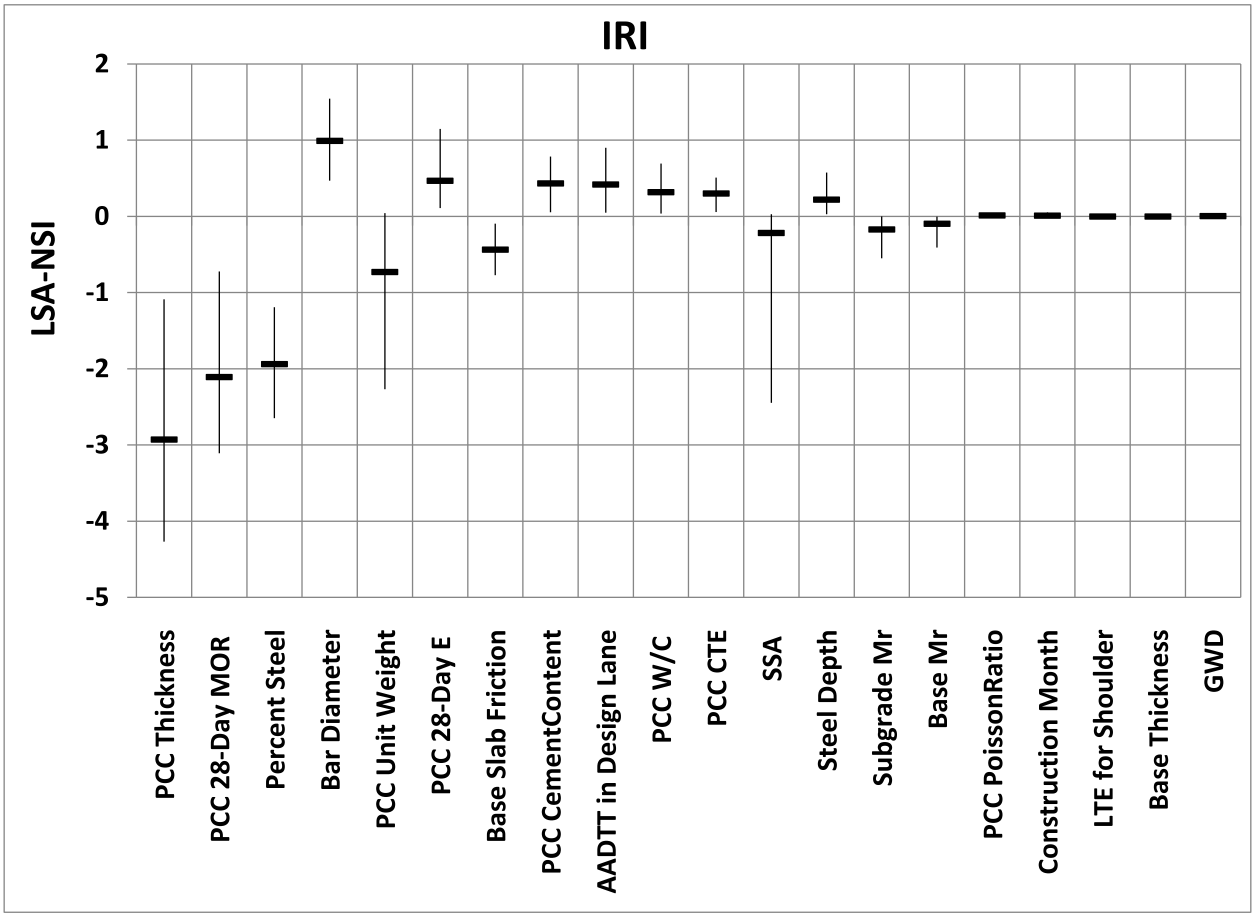

Fig. 3. LSA-NSI values for IRI in CRCP.

5. GSA methodology for MEPDG

Fig. 4 is a schematic of the overall GSA used in this study. Similar to OAT LSA, a set of base cases were made to cover the ranges of commonly encountered pavement types, climate conditions and traffic levels. The GSA also utilized all of MEPDG CRCP inputs used in the OAT LSA (See table 2). However, the GSA considered correlations among MEPDG inputs where appropriate. In addition to this, the GSA varied all inputs simultaneously across the entire problem domain while the OAT LSA varied each input independently by changing baseline, minimum, and maximum values of each design input.

Latin Hypercube Sampling (LHS) was adopted for generating the GSA simulation inputs. Since the GSA simulations provided predictions of pavement performance at random discrete locations in the problem domain, fitting a continuous response surface model (RSM) to the randomly located GSA simulation were developed to compute sensitivity indices at each point in problem domain. Sensitivity index statistics from computed sensitivity indices at each point were utilized to quantify level of sensitivity. Note that OAT LSA utilized sensitivity index at a reference point. The GSA procedure is discussed in detail in the next subsection.

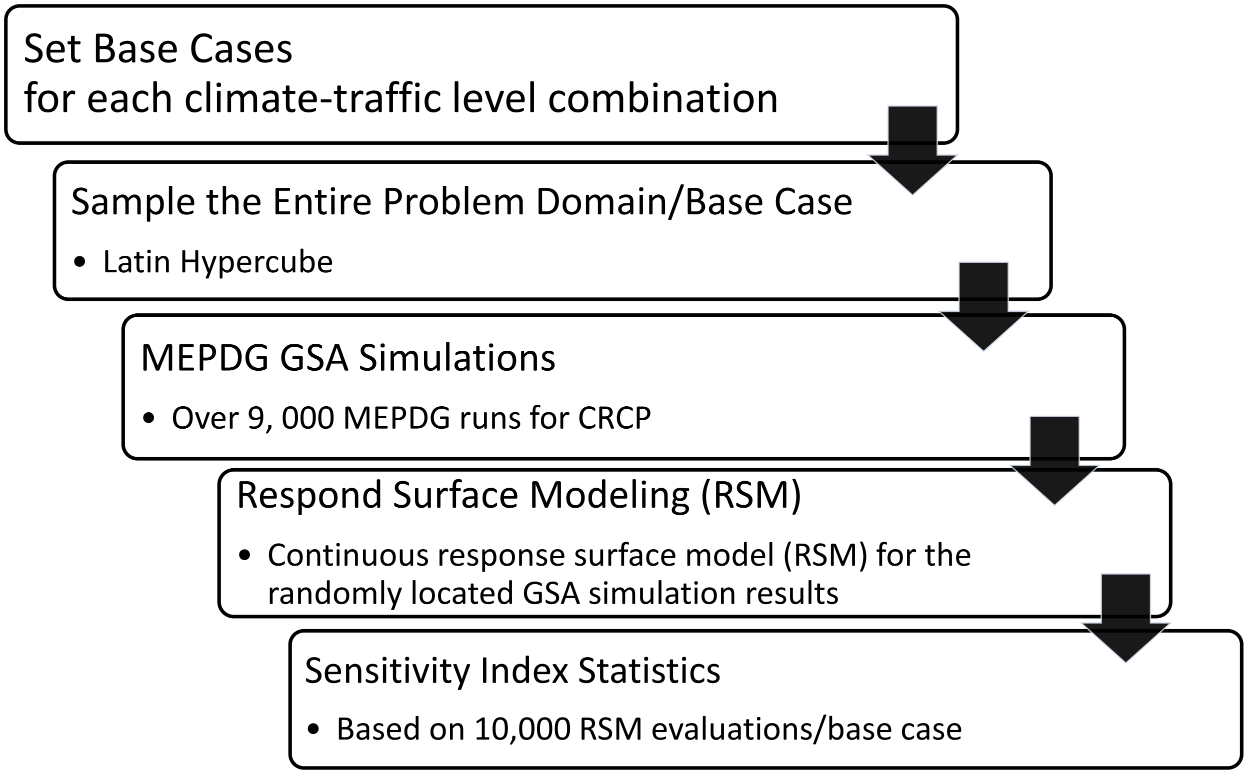

Fig. 4. The schematic of the overall GSA approach.

5.1. Base cases and analysis inputs

Similar to OAT LSA, a total of 15 base cases was developed to cover the ranges of commonly encountered five climatic conditions (See Table 1(a)) and three traffic levels (See Table 1 (b)) with associated CRCP thickness. The GSA varied simultaneously all MEPDG CRCP design inputs utilized in the OAT LSA (See Table 2). The minimum and maximum values are listed for each input assuming uniform distribution. Each input was varied uniformly over each sampling interval between the minimum and maximum limits for generating the GSA simulations.

5.2. Considerations of special input correlations for GSA

Some of the MEPDG inputs are correlated and/or have other characteristics that warrant special treatment. In the GSA simulations, synthetic Level 1 concrete strength and stiffness inputs were generated. Level 1 design inputs require more measurements for the highest accuracy rather than Level 3 design inputs used in OAT LSA. The baseline values of PCC MOR, E, and ITS at various ages were determined from references of 28-day MOR and 28-Day E following the concepts in the MEPDG PCC strength-age correlations. The values for PCC MOR and E at various ages were varied by $\pm$10% about the baseline values to permit evaluation of the sensitivity of predicted performance caused by deviations from the assumptions in the MEPDG PCC strength-age correlations.

The baseline values for the correlated unbound material properties of the percent passing no. 200 sieve (P_{200}), grain diameter at 60% passing (D_{60}), plasticity index (PI), and liquid limit

(LL) were determined from the M_r values using the procedures described in previous studies [10, 11]. The determined values for P200, D_{60}, PI, and LL were varied by $\pm$10% about the baseline values to reflect less-than-perfect correlation with M_r.

The values of W/C ratio were determined from the correlation with PCC strength and the values of steel depth were determined from the correlation with PCC thickness. Similar to OAT LSA, shoulder types for edge support conditions in MEPDG CRCP analyses are equivalent to LTE. More details about these special input considerations are provided in Schwartz et al.[4].

5.3. Latin hypercube sampling for GSA

The GSA requires some form of Monte Carlo simulation to examine the entire parameter space. LHS was adopted for generating the GSA simulation inputs. The LHS is a widely used variant of the standard or "random" Monte Carlo method. In LHS the range of each of the K model inputs X_1, X_2,…, X_K is divided into N intervals in such a way that the probability of the input value falling in any of the intervals is $1/N$. One value is selected at random from each interval. The N values for X_1 are paired randomly with the N values of X_2; these sets are then paired randomly with the N values of X_3 and so on. The resulting $N\times K$-tuples are the LHS samples for the GSA. This process can be repeated with a different random seed to generate as many sets of $N\times K$-tuples as desired. Further details of the LHS sampling procedure are provided in Stein [12].

The efficiency of the LHS approach reduces the required number of simulations by a factor of 5 to 20 compared to the conventional Monte Carlo method while still retaining complete coverage of the input space. There are few guidelines for determining the number of LHS simulations ($N\times K$) required for any given problem. Minimum numbers of simulation samples suggested in the literature include: $4/3\times K$ [13], $3/2\times K$ [14], and $2\times K$ [15], where K is the number of model inputs. Suggested upper bounds for the numbers of simulation samples include: $3\times K$ [16] and $10\times K$ [6, 14, 17].

In reality, both the lower and upper bounds for the number of simulations are dependent upon the specific problem and on the intended use of the simulation results. A limited parametric investigation suggested that sufficiently stable results could be obtained from approximately 400 to 500 simulations per each base case, or approximately $20\times K$ [9]. This is expected to be conservative, as it substantially exceeds even the highest numbers cited in the literature, e.g., $10\times K$ [6, 14, 17]. More details and examples about LHS procedures to MEPDG inputs are provided in Schwartz et al. [4].

5.4. MEPDG GSA simulations

The GSA required many thousands of MEPDG simulation runs demanding the manual entry of all input data. The *AutoIt* scripting utility (http://www.autoitscript.com/autoit3/index.shtml) was adopted to automate the entry/creation of MEPDG input files, to initiate the MEPDG execution, and to collect the analysis results into a central spreadsheet repository. *AutoIt* is a free, open source, sophisticated BASIC-like scripting language designed for automating Windows program operations via simulated keystrokes and mouse movements. *AutoIt* scripts are compiled into stand-alone executable that can be easily distributed and run on other host computers. Over 9,000 MEPDG runs were performed for the CRCP GSA.

Reference to this paper should be made as follows: Ceylan, H., Kim, S., Gopalakrishnan, K., Schwartz, C. W., and Li, R. (2014). "*Sensitivity Analysis Frameworks for Mechanistic-Empirical Pavement Design of Continuously Reinforced Concrete Pavements*," Construction and Building Materials. Vol. 73, pp. 498–508.

For illustration, Fig. 5 provides frequency distributions of CRCP predicted distresses for each of the traffic category (low, medium, and high) under cold-dry climate zone. The range of predicted distresses in most cases is from zero or near zero to three times values of the default design limits. These results confirm that the GSA simulations for the CRCP cases span a wide range of the model output (distress) space as well as the model inputs domain.

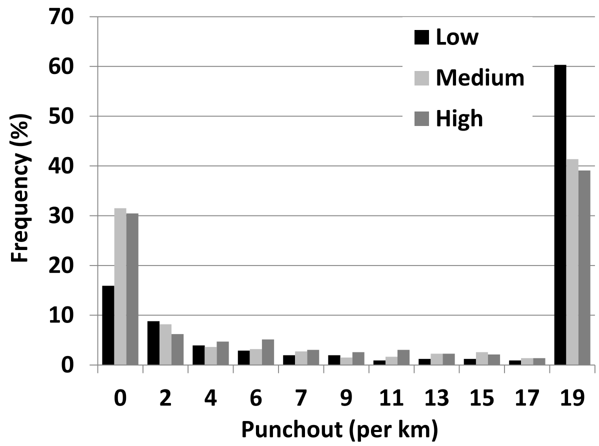

(a)

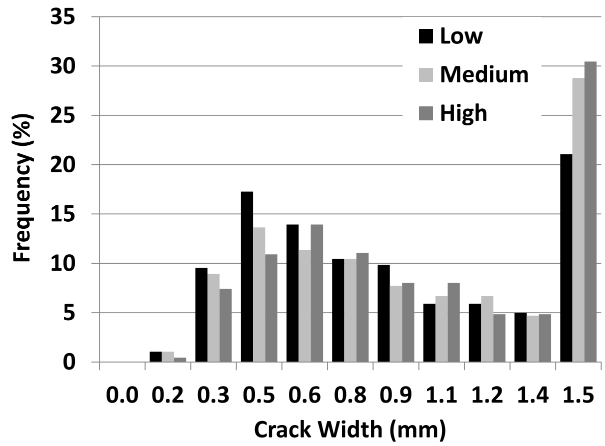

(b)

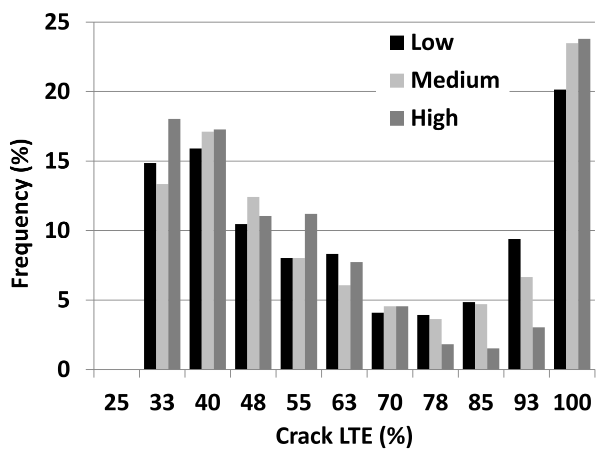

(c)

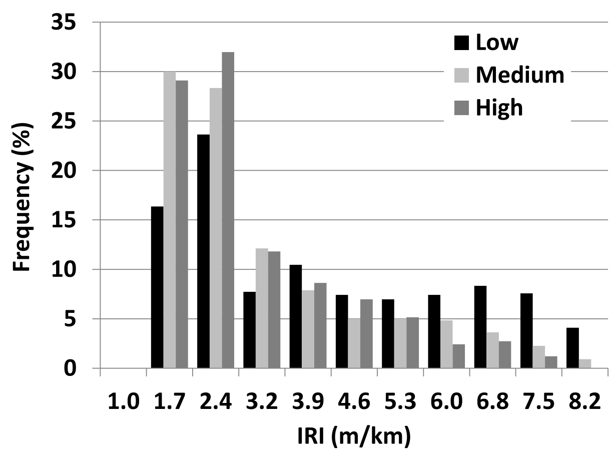

(d)

Fig. 5. Distribution of CRCP predicted distresses under cold-dry (CD) climate zone: (a) punchout, (b) crack width, (c) crack LTE, and (d) IRI.

5.5. RSMs for GSA

The GSA simulations provided predictions of pavement performance at random discrete locations in the problem domain. In order to compute GSA sensitivity indices as defined in next subsection, it is necessary to evaluate the derivatives of distress with respect to inputs at specific discrete locations. Fitting a continuous response surface modeling (RSM) to the randomly located GSA simulation results makes this possible. The derivatives can either be expressed analytically from the RSM or estimated numerically using finite difference approximations in terms of the values of the RSM in the local area around the discrete specified locations.

Two RSM approaches were employed in this study: multivariate linear regressions (MVLR) and artificial neural networks (ANN or NN). MVLR estimates the linear functional trends between model outputs (i.e., individual distresses) and model inputs (i.e., a set of MEPDG inputs). ANN, in contrast, provides a "function-free" numerical approximation of the nonlinear relationship between distresses and MEPDG inputs.

The MVLR is defined in normalized terms as follows:

$$\frac{Y_j}{DL_j} = a_0 + \sum_{i=1}^{n} a_i \frac{X_i}{\overline{X}_i} \qquad (2)$$

in which Y_j is distress j (e.g., faulting), DL_j is the design limit for distress j (e.g., 0.12 in or 3.05 mm for faulting), X_i is MEPDG input i, $\overline{X}_i$ is the mean value of X_i, a_0 is the intercept, and the a_i values are regression coefficients. The regression coefficients represent the average sensitivity of the normalized distress to the normalized input i.

ANN is a newer technique compared to MVLR but has today become a standard data fitting tool for problems that are too complex, poorly understood, or resource-intensive to tackle using more traditional numerical and/or statistical techniques. They can, in a certain sense, be viewed as similar to nonlinear regression except that the functional form of the fitting equation does not need to be specified *a priori*. The basic concepts underlying standard backpropagation ANN can be found in Ceylan et al. [18]. The ANNs in this study were designed, trained, and evaluated using the MATLAB Neural Networks toolbox [19].

All ANNs employed were conventional two-layer (1 hidden layer and 1 output layer) feed-forward backpropagation-type networks. ANN RSMs scenarios employed 23 input neurons, 5 hidden neurons in one layer, and one output neuron. Sigmoid transfer functions were used for all hidden layer neurons while linear transfer functions were employed for the output neurons. Training was accomplished using the Levenberg-Marquardt backpropagation algorithm. Separate ANN models were developed for each distress-climate zone combination. Seventy percent of the GSA simulations for each distress-climate zone combination were used for training, 15% were used for validation (to halt training when generalization stops improving), and the remaining 15% were used for independent testing of the trained model.

5.6. Sensitivity metrics for GSA

The primary metric used for the GSA evaluation is a point-normalized sensitivity index from ANN modeling. Since the values of regression coefficients, a_i , from MVLR are fixed quantities, they cannot capture sensitivity variations at different locations within the problem domain. The a_i values can provide only the average sensitivities over the problem domain.

The nonlinear fitting from the ANN models, on the other hand, can provide point estimates of sensitivities across the problem domain. The point-normalized sensitivity index, S_{ijk}, is defined as:

$$S_{ijk} = \left.\frac{\partial Y_j}{\partial X_k}\right|_i \left(\frac{X_{ki}}{Y_{ji}}\right) \tag{3}$$

in which Y_{ji}, X_{ki} are the values of the model output j and input k all evaluated at location i in the problem domain. The partial derivative can be approximated using a standard central difference approximation:

$$\left.\frac{\partial Y_j}{\partial X_k}\right|_i \cong \left.\frac{\Delta Y_j}{\Delta X_k}\right|_i = \frac{Y_{j,i+1}-Y_{j,i-1}}{X_{k,i+1}-X_{k,i-1}} \tag{4}$$

The S_{ijk} sensitivity index can be interpreted as the local percentage change in model output Y_j caused by a given percentage change in the model input X_k at location i in the problem domain. For example, $S_{ijk} = 0.5$ implies that a 20% change in the local value of X_{ki} will cause a 10% local change in Y_{ji}. Since S_{ijk} is a local point estimate of sensitivity, it will vary across the problem domain.

Problems were encountered when calculating the point-normalized sensitivity index for some analyses because the predicted distress values Y_{ji} (denominator in Eq. 3) were near zero for some of the input sets, resulting in artificially large sensitivity index values. To circumvent this problem, a "design limit" *NSI* of S_{ijk}^{DL} for GSA, similar to OAT LSA, was defined as:

$$S_{ijk}^{DL} = \left.\frac{\Delta Y_j}{\Delta X_k}\right|_i \left(\frac{X_{ki}}{DL_j}\right) \tag{5}$$

in which X_{ki} is the value of input k at point i, ΔX_{ki} is the change in input k about point i, ΔY_{ji} is the change in predicted distress j corresponding to ΔX_{ki}, and DL_j is the design limit for distress j. For simplicity, the design limit normalized sensitivity index, S_{ijk}^{DL} is termed more simply as the "GSA normalized sensitivity index" or *GSA-NSI*. *GSA-NSI* can be interpreted in a similar way to *LSA-NSI* as the percentage change in predicted distress relative to the design limit caused by a given percentage change in the design input.

6. GSA results

6.1. RSM results

The inputs used for the CRCP RSMs are AADTT per design lane, PCC slab thickness, base layer thickness and the other 20 MEPDG inputs listed in Table 2. The outputs for the RSMs are the predicted distresses: punchout, crack width, crack LTE, and IRI at the end of the 25-year service life. Separate RSMs were developed for each distress and climate combination.

Goodness-of-fit statistics such as the coefficient-of-determination (R^2) and normalized standard error (Se/Sy) for the both MVLR RSMs and ANN RSMs are summarized in Table 4 by climate zone and distress. The R^2 of MVLR RSMs values range from about 0.5 to 0.8, with the crack width tending to have smaller R^2 values and the punchout, crack LTE, and IRI distresses tending to have relatively better goodness-of-fit statistics. The low R^2 values for many of the

MVLR RSMs indicate that the MVLR RSMs, although widely employed in the sensitivity analysis literature, are insufficient for capturing the complex nonlinearities of pavement performance.

Table 4. Goodness-of-fit Statistics for RSMs.

Climate	Distress	MVLR RSMs		ANN RSMs	
		R^2	Se/Sy	R^2	Se/Sy
CD	Punchout	0.73	0.52	0.93	0.27
	Crack Width	0.54	0.68	0.94	0.24
	Crack LTE	0.77	0.48	0.89	0.33
	IRI	0.74	0.52	0.90	0.31
CW	Punchout	0.72	0.53	0.92	0.28
	Crack Width	0.54	0.68	0.95	0.23
	Crack LTE	0.77	0.48	0.90	0.31
	IRI	0.75	0.51	0.91	0.30
T	Punchout	0.70	0.55	0.94	0.25
	Crack Width	0.55	0.68	0.93	0.26
	Crack LTE	0.75	0.51	0.88	0.34
	IRI	0.70	0.55	0.92	0.28
HD	Punchout	0.73	0.52	0.94	0.24
	Crack Width	0.58	0.65	0.96	0.20
	Crack LTE	0.78	0.47	0.93	0.26
	IRI	0.73	0.52	0.95	0.23
HW	Punchout	0.71	0.54	0.93	0.26
	Crack Width	0.58	0.65	0.97	0.16
	Crack LTE	0.77	0.49	0.88	0.34
	IRI	0.71	0.54	0.91	0.31

Overall, the ANN RSM model fits are excellent with the lowest one being 0.88 for crack LTE. Scatter plots for ANN predicted vs. MEPDG predicted distresses under cold-dry climate condition are provided in Fig. 6 for illustration. These scatter plots graphically confirm the conclusions from the goodness-of-fit statistics that the ANN RSM models provide excellent fits. The high quality of the fits for these ANN RSMs suggest the possibility that enhanced versions of the RSM might be adequate substitutes in some cases for the more rigorous but laborious geomechanics computations in the MEPDG.

Reference to this paper should be made as follows: Ceylan, H., Kim, S., Gopalakrishnan, K., Schwartz, C. W., and Li, R. (2014). "*Sensitivity Analysis Frameworks for Mechanistic-Empirical Pavement Design of Continuously Reinforced Concrete Pavements*," Construction and Building Materials. Vol. 73, pp. 498–508.

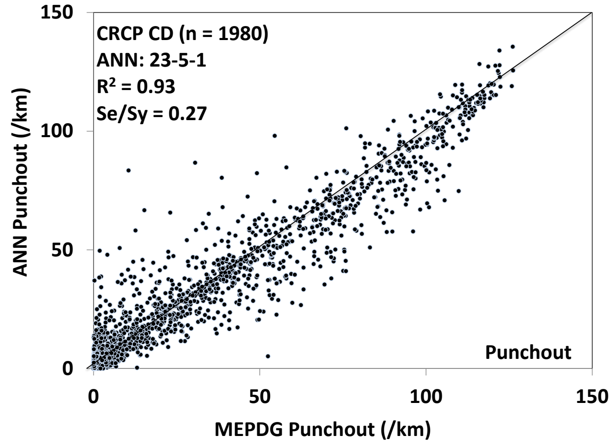

(a)

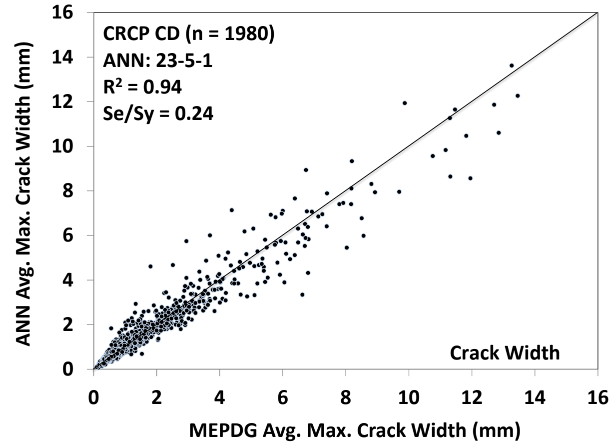

(b)

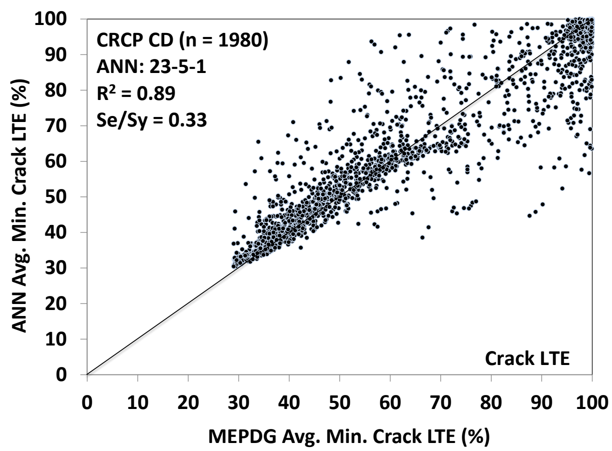

(c)

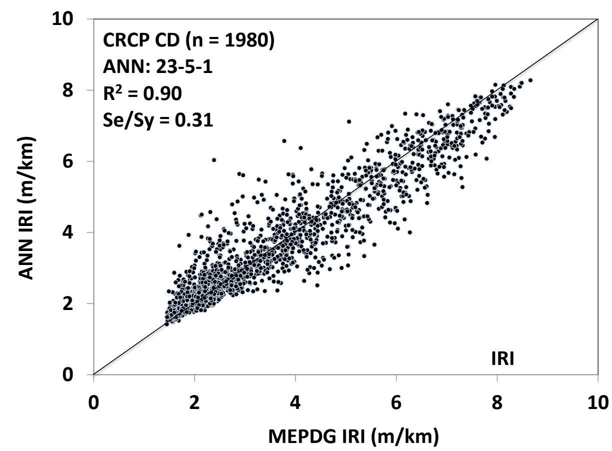

(d)

Fig. 6. ANN predicted vs. MEDPG predicted CRCP distresses under cold-dry (CD) climate zone: (a) punchout, (b) crack width, (c) crack LTE, and (d) IRI.

6.2. Sensitivity index statistics results

The ANN RSMs permit a more in-depth evaluation of sensitivities than does the MVLR approach. Ten thousand ANN RSMs were performed for each climate zone and distress combination using random sampling of all inputs across the problem domain. Full frequency distributions of the computed GSA-NSI values and summary statistics (minimum, maximum, mean, standard deviation, etc.) by input and climate zone were depicted and documented in Schwartz et al. [4]. For sake of illustration, Fig. 7 illustrates some representative frequency distributions of the computed GSA-NSI values for each performance prediction under the different climate zones (CD, CW, T, HD, and HW).

An important feature to note in the frequency distributions is that most have well-defined peaks: this implies that the GSA-NSI values are close to the mode at nearly all locations in the

Reference to this paper should be made as follows: Ceylan, H., Kim, S., Gopalakrishnan, K., Schwartz, C. W., and Li, R. (2014). "*Sensitivity Analysis Frameworks for Mechanistic-Empirical Pavement Design of Continuously Reinforced Concrete Pavements*," Construction and Building Materials. Vol. 73, pp. 498–508.

problem domain—i.e., GSA-NSI does not vary significantly over the problem domain. The influence of climate zone on the frequency distributions is also negligible in most cases.

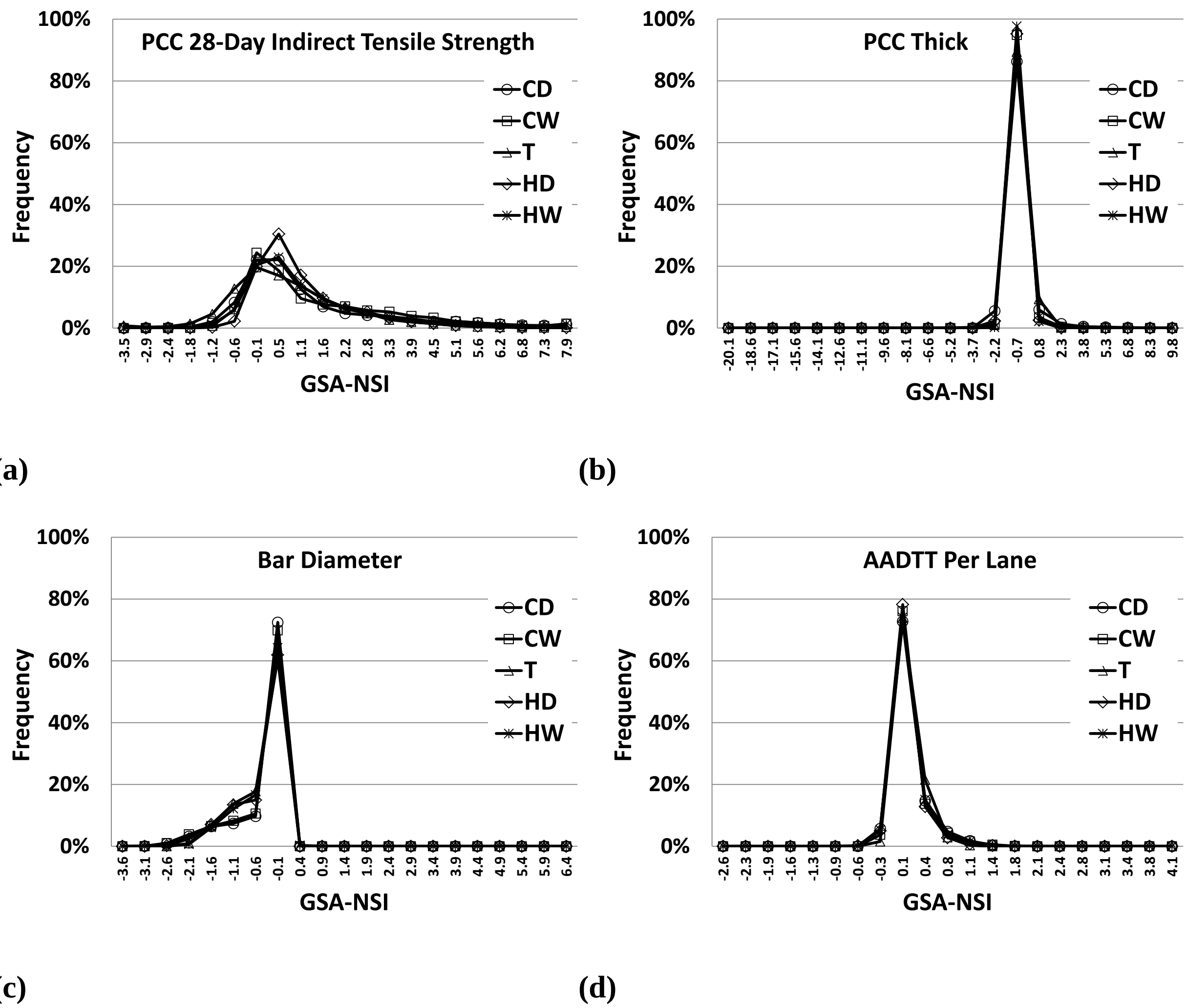

Fig. 7. Distributions of GSA-NSI values for JPCP: (a) punchout by PCC 28-Day indirect tensile strength, (b) crack width by PCC thickness, (c) crack LTE by bar diameter, and (d) IRI by AADTT per lane.

7. Discussions

The CRCP design inputs are listed in Table 5 in rank order by the maximum absolute value of mean plus/minus two standard deviation ($\mu \pm 2\sigma$) GSA-NSI values computed using the statistics based on the 10,000 ANN RSM evaluations for each climate zone and distress combination. The $\mu \pm 2\sigma$ GSA-NSI metric (GSA- $NSI_{\mu \pm 2\sigma}$) captures both the mean value of the sensitivity and the range of sensitivity across the problem domain. The plus and minus signs are retained for each individual sensitivity index to indicate whether distress increases (+) or decreases (-) with increasing input value.

The OAT LSA category based on the maximum value of LSA-NSI for each MEPDG input is also indicated in Table 5. These sensitivity categories, as defined for the OAT LSA analysis results, are highlighted by the fonts of GSA- $NSI_{\mu\pm2\sigma}$ values in Table 5: **Bold** = Hypersensitive (HS), GSA- $NSI_{\mu\pm2\sigma}$ > 5; ***Bold Italic*** = Very Sensitive (VS), 1 < GSA- $NSI_{\mu\pm2\sigma}$ < 5; *Italic* = Sensitive (S), 0.1 < GSA- $NSI_{\mu\pm2\sigma}$ < 1; and Regular = Non-Sensitive (NS), GSA-$NSI_{\mu\pm2\sigma}$ < 0.1. The heavy lines in the table indicate the break points between GSA sensitivity categories. For added insight, the top three GSA sensitivity values for each distress are indicated by the shaded cells in the table.

Not only is there good congruence between the ranking of inputs from the GSA and the categorization from the OAT LSA analyses, but the ranges of GSA-$NSI_{\mu\pm2\sigma}$ in Table 5 also line up closely with the ranges of *LSA-NSI* used to define the OAT LSA categories. At GSA-$NSI_{\mu\pm2\sigma}$ = 1 corresponding to the upper limit of the Sensitive range in Table 5, the percentage change in distress relative to its design limit equals the percentage change in the MEPDG input. This is very small in practical terms, especially since it is defined at the $\mu\pm2\sigma$ level. The focus of the pavement designer should therefore be on the Hypersensitive and Very Sensitive MEPDG inputs; these are the values that need to be most carefully determined. The rankings and GSA-$NSI_{\mu\pm2\sigma}$ values in Table 5 are judged to be the good measures of the MEPDG input sensitivities in the MEPDG. The graphical summaries of the input sensitivities by distress are available in Schwartz et al. [4].

These results match engineering judgment and experience in overall terms. Although the details vary by distress type, most of the highest sensitivity design inputs are PCC layer properties (PCC thickness, PCC strength parameters, reinforcing steel properties, PCC unit weight, PCC coefficient of thermal expansion, surface shortwave absorptivity) followed by the base and subgrade properties. Traffic volume is also an important design input. However, there are a few observations that merit special note and discussion:

- The largest sensitivity values for CRCP are substantially larger than those for any of the other pavement types.
- The magnitudes (mean and standard deviation) of the highest sensitivity values for punchouts and crack width are substantially greater than the values for crack LTE and IRI.
- The sensitivity index values for each distress-design input combination do not vary substantially or systematically by climate zone.

Reference to this paper should be made as follows: Ceylan, H., Kim, S., Gopalakrishnan, K., Schwartz, C. W., and Li, R. (2014). "*Sensitivity Analysis Frameworks for Mechanistic-Empirical Pavement Design of Continuously Reinforced Concrete Pavements*," Construction and Building Materials. Vol. 73, pp. 498–508.

Table 5. Ranking of MEPDG CRCP inputs by maximum GSA-NSI$_{\mu\pm2\sigma}$ values (ANN RSMs).

Design Input	**Maximum GSA-NSI$_{\mu\pm2\sigma}$ Values (ANN RSMs)[1] for GSA**					**OAT-LSA[2]**
	Punchout	**Crack Width**	**Crack LTE**	**IRI**	**Max**	
PCC 28-Day Indirect Tensile Strength	**11.13**	**61.48**	***-1.33***	***2.37***	**61.48**	-[3]
PCC 28-Day Modulus of Rupture	**-40.29**	**-47.80**	***2.35***	**-7.37**	**-47.80**	**HS**
PCC Thickness	**-44.43**	**-10.47**	***1.57***	**-8.94**	**-44.43**	**HS**
PCC Water-to-Cement Ratio	**8.42**	**36.09**	*-0.82*	***1.88***	**36.09**	**HS**
PCC Unit Weight	**-17.22**	**-35.27**	*0.53*	***-3.22***	**-35.27**	**HS**
Bar Diameter	**11.41**	**23.29**	***-1.49***	***1.93***	**23.29**	**HS**
Base Slab Friction	***-4.17***	**-21.62**	*0.35*	*-0.78*	**-21.62**	**HS**
PCC Cement Content	**7.56**	**21.55**	*-0.65*	***1.38***	**21.55**	**HS**
PCC Ratio 20-year to 28-day Modulus of Rupture	**-18.81**	**7.88**	*-0.50*	***-3.48***	**-18.81**	-[3]
Percent Steel	**-15.41**	**-18.00**	***1.04***	***-2.99***	**-18.00**	**HS**
PCC 28-Day Elastic Modulus	**10.90**	**15.97**	*-0.61*	***2.13***	**15.97**	**HS**
Steel Depth	**6.43**	**13.39**	*-0.61*	***1.51***	**13.39**	**HS**
Traffic Volume (AADTT)	**8.47**	***1.03***	*-0.42*	***1.61***	**8.47**	**HS**
Base Resilient Modulus	**-6.39**	***-4.71***	*0.10*	***-1.16***	**-6.39**	***VS***
PCC Coef. of Thermal Expansion	**6.19**	**5.54**	-0.06	***1.19***	**6.19**	***VS***
PCC Ratio 20-year to 28-day Indirect Tensile Strength	***1.62***	**-5.81**	*0.14*	*-0.29*	**-5.81**	-[3]
Surface Shortwave Absorptivity	***3.32***	**-5.44**	*0.20*	*0.74*	**-5.44**	**HS**
Base Thickness	***-1.79***	***4.71***	*-0.10*	*-0.42*	***4.71***	*S*
Subgrade Resilient Modulus	***-3.23***	***-4.64***	0.06	***-1.17***	***-4.64***	***VS***
Edge Support – Load Transfer Efficiency	***-3.26***	***2.16***	*0.30*	*-0.59*	***-3.26***	*S*
PCC Poisson's Ratio	***1.79***	***-2.44***	0.04	*0.34*	***-2.44***	*S*
Construction Month	***1.62***	***2.33***	-0.08	*0.25*	***2.33***	*S*
Groundwater Depth	*0.43*	***-1.19***	0.03	-0.09	***-1.19***	*S*

[1]Maximum sensitivity (in absolute value sense) over all baseline cases and distresses. Sensitivity ratings are indicated by font type: **Bold** designates Hypersensitive, NSI$_{\mu\pm2\sigma}$ > 5; ***Bold Italics*** designates Very Sensitive, 1 < NSI$_{\mu\pm2\sigma}$ < 5; *Italics* designates Sensitive, 0.1 < NSI$_{\mu\pm2\sigma}$< 1; and Regular font designates Insensitive, NSI$_{\mu\pm2\sigma}$ < 0.1. Bold lines indicate breaks between sensitivity categories. Shaded entries indicate the three most sensitive inputs for each individual distress.
[2]HS=Hypersensitive; VS=Very Sensitive; S=Sensitive; NS=Non-Sensitive.
[3]20-year strength ratio values not considered explicitly in OAT LSA analyses.

8. Conclusions and recommendations

Extensive local sensitivity analyses (LSA) based on one-at-time (OAT) method and comprehensive global sensitivity analyses (GSA) are proposed and conducted to evaluate the sensitivity of MEPDG CRCP performance predictions to design inputs. The major conclusions and recommendations drawn from the developed LSA and GSA methodology and results are summarized below:

- The design limit normalized sensitivity index (NSI) adopted in OAT LSA and GSA has the practical interpretation of relating a given percentage change in a MEPDG input to the corresponding percentage change in predicted distress relative to its design limit value.
- The artificial neural network (ANN) response surface models (RSMs) adapted in GSA provided generally robust and accurate representations of the complex relationships between MEPDG inputs and distress outputs. The ANNs achieved good goodness-of-fit statistics for all of MEPDG CPRP performance predictions. The ANN RSMs capture the variation of sensitivities across the problem domain and thus enabled generation of frequency distributions and summary statistics (minimum, maximum, mean, standard deviation, etc.). Enhanced versions of the ANN RSMs (e.g., to include climate effects more explicitly) could in some cases be adequate replacements for the more rigorous but laborious geomechanics computations in the MEPDG.
- The "mean plus/minus two standard deviations (μ+2σ)" GSA-NSI metric (GSA-NSI$_{\mu\pm2\sigma}$) derived from ANN RSM statistics was judged to be the best and most robust ranking measure because it incorporates both the mean sensitivity and the variability of sensitivity across the problem domain.
- The multivariate linear regression (MVLR) RSMs, although widely employed in the sensitivity analysis literature, were insufficient for capturing the complex nonlinearities of pavement performance. The MVLR RSMs in this study had only poor to fair goodness-of-fit statistics.
- The design input rankings by GSA-NSI$_{\mu\pm2\sigma}$ agreed well with the OAT LSA rankings by *LSA-NSI*. This should not be interpreted as implying that OAT LSA will be an acceptable substitute for the more demanding GSA. Rather, it is due in large part to the exhaustive nature of the OAT LSA considered in this study. The set of 585 MEPDG analyses over 5 pavement types, 5 climate zones, 3 traffic levels, and dozens of design inputs sampled a significantly larger subset of the problem domain than in most past studies. The OAT LSA rankings were also based on the very severe metric of the maximum NSI value observed for any distress, pavement type, climate zone, or traffic level. This is similar in concept (although not in detail) to the NSI$_{\mu\pm2\sigma}$ metric in the GSA.
- Most of the consistently highest sensitivity design inputs were reinforced PCC/steel layer properties (PCC thickness, PCC strength and stiffness properties, reinforcing steel properties, PCC unit weight, PCC coefficient of thermal expansion) followed by the base and subgrade properties. Traffic volume was also an important design input.
- The magnitudes (mean and standard deviation) of the highest sensitivity values for punchouts and crack width were substantially greater than the values for crack LTE and IRI.

- The sensitivity values for each distress-design input combination did not vary substantially or systematically by climate zone. However, the distress magnitudes may vary across climate zones.
- Guidance for the pavement designer on how to address high sensitivity or critical design inputs varies depending upon the specific design input. Some high sensitivity inputs can be specified very precisely, e.g., PCC thickness and the steel properties. Other inputs need to be measured or estimated. The high sensitivity of performance to the PCC strength and stiffness properties indicates a need for careful characterization of these values. Mix-specific laboratory measurement of Level 1 PCC modulus of rupture, indirect tensile strength, and modulus of elasticity may be appropriate for high-value projects. Other properties like the PCC ratio 20-year to 28-day modulus of rupture and PCC coefficient of thermal expansion are very difficult to measure, and testing protocols are still evolving. For this as well as all other high sensitivity design inputs, the pavement designer should perform project-specific design sensitivity studies to evaluate the consequences of uncertain input values.

Acknowledgements

The authors gratefully acknowledge the National Cooperative Highway Research Program (NCHRP) of the Transportation Research Board (TRB) for supporting this study. The authors are also grateful to Dr. Amir N. Hanna and NCHRP 1-47 Project technical panel members for their timely review and valuable comments. The contents of this paper reflect the views of the authors who are responsible for the facts and accuracy of the data presented within. The contents do not necessarily reflect the official views and policies of the TRB. This paper does not constitute a standard, specification, or regulation

References

[1] American Association of State Highway and Transportation Officials [Internet]. AASHTOWare Pavement ME Design [cited 2014 August 12]. Available from: http://www.aashtoware.org/Pavement/Pages/default.aspx.

[2] National Cooperative Highway Research Program. Guide for mechanistic-empirical design of new and rehabilitated pavement structures. Final Report of NCHRP Project 1-37A, Washington, DC: Transportation Research Board, National Research Council; 2004.

[3] American Association of State Highway and Transportation Officials. Mechanistic-empirical pavement design guide, interim edition: a manual of practice. Washington, DC: AASHTO; 2008.

[4] Schwartz CW, Li R, Kim, S, Ceylan, H, Gopalakrishnan, K. Sensitivity evaluation of MEPDG performance prediction. Final Contractor Report of NCHRP 1-47, Washington, DC: Transportation Research Board, National Research Council; 2011.

[5] Cacuci DG. Sensitivity and uncertainty analysis theory: volume I. Boca Raton, FL: Chapman and Hall/CRC; 2003.

[6] Saltelli A, Tarantola S, Campolongo F, Ratto M. Sensitivity analysis in practice. Chichester, England: John Wiley & Sons; 2004.

[7] Alam M, Fekpeet E, Majed M. FHWA FAF^2 freight traffic analysis report [Internet]. Washington, DC: Federal Highway Administration; 2007 [cited 2014 August 12]. Available from: http://ops.fhwa.dot.gov/freight/freight_analysis/faf/faf2_reports/reports7/.

[8] Mallela J, Titus-Gover L, Ayers ME, Wilson TP. Characterization of mechanical properties and variability of PCC materials for rigid pavement design. In Seventh International Conference on Concrete Pavements: The use of concrete in developing long-lasting pavement solutions for the 21st century; 2001 September 20-24; Orlando, FL. International Society for Concrete Pavements; 2001, Vol. I, p. 259-279.

[9] Schwartz CW, Li R, Kim S, Ceylan H, Gopalakrishnan K. Effect of PCC strength and stiffness characterization on MEPDG predicted performance of JPCP structures. Transportation Research Record 2011; 2226: 41-50.

[10] Schwartz CW, Li R. Sensitivity of predicted flexible pavement performance to unbound material hydraulic properties. In: Fratta DO, Puppala AJ, Muhunthan B, editors. GeoFlorida 2010: Advances in analysis, modeling, and design, Geotechnical Special Publication 199; 2010 February 20-24; Orlando, FL. VA: ASCE; 2010, p.2672-.2683.

[11] Li R, Schwartz CW, Kim S, Ceylan H. Local Sensitivity of mechanistic-empirical flexible pavement performance predictions to unbound material property inputs. In: Hryciw RD, Athanasopoulos-Zekkos A, Yesiller N, editors. Proceedings of GeoCongress 2012: State of the art and practice in geotechnical engineering [CD-ROM]; 2012 March 25-29; Oakland, CA. VA: ASCE; 2012.

[12] Stein M. Large sample properties of simulations using Latin Hypercube Sampling. Technometrics 1987; 29 (2): 143-151.

[13] Iman RL, Helton JC. A comparison of uncertainty and sensitivity analysis techniques for computer models. Report No. NUREG/CR-3904, Albuquerque, NM: Sandia National Laboratories; 1985.

[14] Simlab Manual [Internet]. Joint Research Centre, Institute for the Protection and Security of the Citizen; [updated 2014 January 8; cited 2014 August 12]. Available from http://ipsc.jrc.ec.europa.eu/?id=756.

[15] McKay MD. Sensitivity and uncertainty analysis using a statistical sample of input values. In: Ronen Y, editor. Uncertainty Analysis, Boca Raton, FL: CRC Press, 1988, p. 145-186.

[16] Manache, G. Sensitivity of a continuous water-quality simulation model to uncertain model input parameters [dissertation]. Belgium: Vrije University of Brussels; 2001.

[17] Graves RC, Mahboub KC. Pilot study in sampling-based sensitivity analysis of NCHRP design guide for flexible pavements. Transportation Research Record 2006; 1947: 123-135.

[18] Ceylan H, Schwartz CW, Kim S, Gopalakrishnan K. Accuracy of predictive models for dynamic modulus of hot mix asphalt. Journal of Materials in Civil Engineering 2009; 21(6): 286-293.

[19] Beale MH, Hagan MT, Demuth HB. Neural Network Toolbox™ user's guide [Internet]. Natick, MA: MathWorks, Inc.; 2011 [cited 2012 May 29]. Available from http://www.mathworks.com/help/pdf_doc/nnet/nnet_ug.pdf .